## Environmental Science Nano



PAPER

View Article Online
View Journal



Cite this: DOI: 10.1039/c9en01007f

# Transport of food- and catalytic-grade titanium dioxide nanoparticles in controlled field streams with varying streambed and biofilm conditions†

Junyeol Kim,<sup>a</sup> Kevin R. Roche,<sup>a</sup> John Sticha,<sup>a</sup> Arial J. Shogren,<sup>b</sup> Diogo Bolster<sup>a</sup> and Kyle Doudrick (1)\*\*a

With the increased use of nanoparticles (NPs) in consumer, food, and pharmaceutical products, their eventual release into streams is inevitable. Critical factors affecting the transport of NPs in streams are the hyporheic exchange between the water column and porous streambed substrate and the interaction with biofilms. In this study, the transport behavior of two titanium dioxide NPs – catalytic– (P90) and food–grade (E171) – was evaluated in four field streams lined with different streambed substrate sizes for varying seasonal biofilm conditions. When biofilm growth was minimal, NP retention in the streams increased with increasing substrate size due to increased hyporheic exchange and subsequent physical and chemical interactions between the NPs and substrate. For all streams, the average mass recovery at the 40 m sampling point for E171 and P90 was  $44 \pm 8.7\%$  and  $16 \pm 8.0\%$ , respectively. The greater mobility of E171 was due to the inherent presence of negatively charged surface phosphates that reduced aggregation and decreased its interaction with the substrate. When biofilms were thriving in the streams the average mass recovery at 40 m for both NPs decreased significantly (E171 =  $5.8 \pm 7.3\%$ , P = 0.0017; P90 =  $2.4 \pm 0.7\%$ , P = 0.041), and the mass recovery difference between the two NPs became insignificant (P = 0.38).

Received 5th September 2019, Accepted 8th October 2019

DOI: 10.1039/c9en01007f

rsc.li/es-nano

#### **Environmental significance**

Titanium dioxide nanoparticles (NPs) are commonly used in consumer, food, and pharmaceutical products and they are likely to enter the environment upon disposal. Identifying how NPs transport in stream networks is critical to understanding their impact on stream ecology. Lab-scale studies cannot accurately describe the complexity of real streams and there is a need for datasets from larger, more realistic scales. This study uses controlled, field-scale streams to evaluate the transport behavior of catalytic- and food-grade NPs as a function of streambed substrate size and biofilm conditions. Outcomes highlight the importance of considering stream-subsurface exchange and the presence of biofilms, which enhance retention in the streams.

#### 1. Introduction

Engineered nanoparticles (NPs) are an emerging class of materials that are commonly found in consumer, food, and pharmaceutical products. <sup>1-4</sup> Upon their release from products, NPs can enter streams directly or indirectly from wastewater treatment plant and landfill discharges. <sup>5,6</sup> While there have been numerous controlled lab-scale studies on the environmental transport of NPs (*e.g.*, porous media column tests), <sup>7-27</sup> experimental data is limited for realistic streams where transport will be controlled by surface flows, subsurface

interactions, and contact with biofilms. This lack of data inhibits our ability to mathematically predict NP transport at scale of environmental interest.

Hyporheic exchange involves the advective and dispersive transfer of water between the stream and the underlying and adjacent subsurface that is composed of complex porous substrate. Suspended (e.g., NPs) or dissolved materials can be carried with the water into the substrate, where physical, chemical, and biological processes can strongly impact their transport.<sup>28,29</sup> Aggregation reactions between NPs (i.e., homoaggregation) and between NPs and collectors such as clays (i.e., heteroaggregation) can result in increased settling rates that lead to enhanced hyporheic exchange and shorter transport lengths.<sup>30–46</sup>

Biofilms are a complex assemblage of algae, bacteria, and fungi embedded in extracellular polymeric substances. They are present in streams and can colonize on the surface of the porous substrate or vegetation or they can be suspended in the

E-mail: kdoudrick@nd.edu; Tel: +1 5746310305

<sup>&</sup>lt;sup>a</sup> Department of Civil and Environmental Engineering and Earth Sciences, University of Notre Dame, Notre Dame, IN 46556, USA.

<sup>&</sup>lt;sup>b</sup> Department of Earth and Environmental Sciences, Michigan State University, East Lansing, MI 48824, USA

 $<sup>\</sup>dagger$  Electronic supplementary information (ESI) available. See DOI: 10.1039/c9en01007f

water column.<sup>47</sup> Biofilms also expected to be a dominant factor controlling downstream transport by immobilizing NPs.<sup>18,48–53</sup> The presence of biofilms has been shown to increase the retention of NPs in the porous substrate<sup>18,49,50,52,53</sup> and the water column.<sup>54</sup> In turn, the accumulation of NPs in biofilms can induce negative effects that impact the stream ecology.<sup>55–59</sup>

Predicting transport of anything in streams is complex due to the multivariate, interconnected processes, and these cannot be accurately described using simplistic lab-scale datasets. Thus, there is a need for controlled field studies that can capture realistic behavior. The objective of this study was to evaluate the transport of NPs in controlled field streams as a function of streambed substrate size and seasonal biofilm growth. All stream experiments were conducted at the University of Notre Dame Linked Experimental Ecosystem Facility (ND-LEEF). The ND-LEEF site has four identical experimental streams, which differ only in the size of the streambed substrate lining the bottom. Titanium dioxide (TiO2) was used as an important and representative NP. TiO2 NPs are commonly used as a white pigment in food and personal care products, designated as food-grade TiO<sub>2</sub> or E171.<sup>60</sup> Most studies investigating the environmental and health implications of TiO<sub>2</sub> NPs have used catalytic-grade TiO<sub>2</sub> (e.g., P25 or P90 from Evonik),61 but using this as a reference material in place of E171 is not suitable<sup>62,63</sup> due to the differences in size distribution and surface chemistry. The surface of E171 is more negatively charged due to the presence of surface phosphates and stark behavioral differences have been observed compared to catalytic-grade TiO2.63-67 In this study, we compared the transport behavior of both E171 and P90, and link their aggregation behavior to observed transport outcomes.

## 2. Methodology

#### 2.1 Nanoparticles and tracers

Two TiO<sub>2</sub> NPs (P90 and E171) were used for the stream transport experiments. P90 was donated by Evonik (Essen,

Germany) and used as received. It is a mixture of anatase (86%) and rutile (14%) with an average primary particle size of 12 nm and 18 nm, respectively. E171 was purchased from Minerals-Water Ltd. (Purfleet, UK) and used as received. E171 is mostly anatase with a particle size range of  $106-132\pm38-56$  nm, depending on the manufacturer. He pH zero point of charge (pH<sub>zpc</sub>) of P90 and E171 in an aqueous solution is approximately 6.0 and 4.5, respectively. The lower pH<sub>zpc</sub> of E171 is attributed to the negatively charged phosphate groups attached to its surface. E151

Potassium bromide (KBr; Fisher Scientific, Hampton, NH, USA) and rhodamine water tracer (RWT, C<sub>29</sub>H<sub>29</sub>ClN<sub>2</sub>Na<sub>2</sub>O<sub>5</sub>; Acros Organics, NJ, USA) were used as conservative tracers in the stream transport experiments. RWT has previously been shown to be suitable for experiments at ND-LEEF,<sup>71–73</sup> and both RWT and KBr were used in this study interchangeably, depending on the season and equipment available. KBr was used as a conservative tracer in June when few biofilms were present. In September, when biofilms were flourishing, RWT was used to accurately resolve adsorption to biofilms and to obtain a wider range of concentrations.

#### 2.2 ND-LEEF site description

Field experiments were conducted in the experimental streams at ND-LEEF, which is located at St. Patrick's County Park in South Bend, IN, USA (Fig. 1A). ND-LEEF is a globally unique research facility that houses two man-made experimental watersheds, each consisting of an interconnected pond, two stream reaches, and a wetland. The four experimental streams are identical in terms of hydraulic gradient, width, and other primary hydraulic characteristics (Fig. S1†). Specifically, each stream is 0.4 m wide and 55 m long with a hydraulic gradient of 0.0075. The stream channel base is lined with cement concrete to prevent uncontrolled hydrologic interactions with the surroundings. Previous studies in these streams have

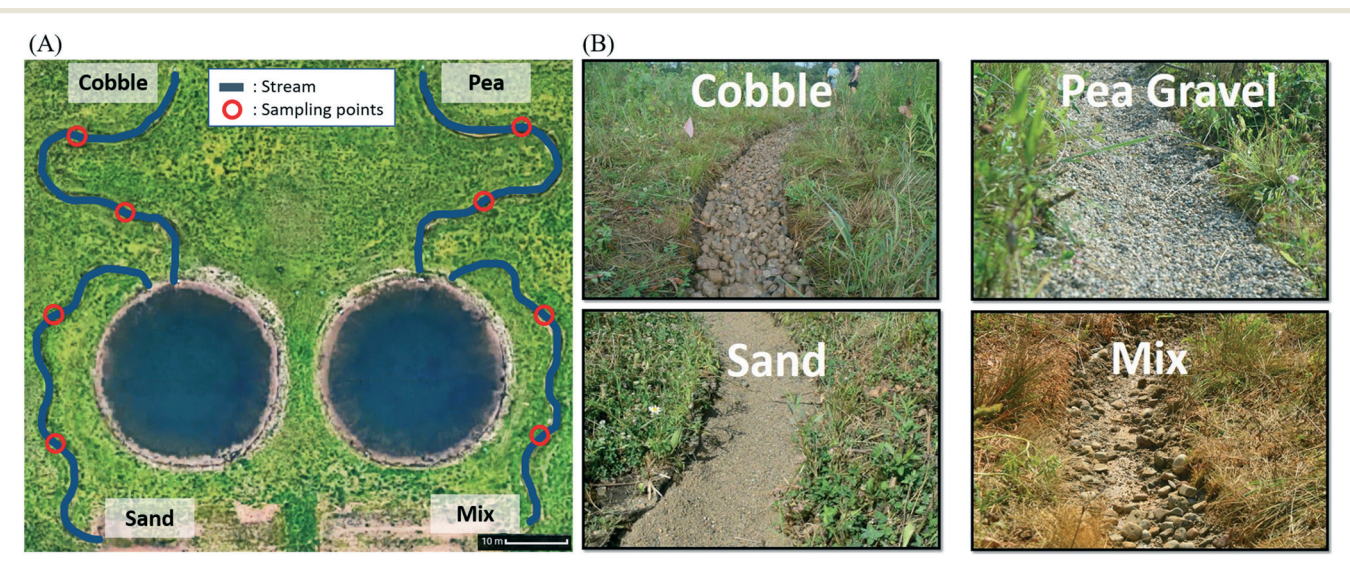


Fig. 1 (A) Aerial photograph of ND-LEEF site (obtained from Google Earth) with schematic detailing stream location and sampling points. (B) Photographs of streambed substrates for each stream.

Environmental Science: Nano Paper

shown that dilution is minimal as there is no lateral inflow of water.74 Each streambed has a unique substrate approximately 10 cm thick. In this study, the streams were lined with sand (sand), pea gravel (pea), cobble gravel (cobble), and a 1:1:1 volume ratio mixture of all three (mix) (Fig. 1B). The average  $D_{50}$  size of the substrates is 0.053 cm, 0.67 cm, and 5 cm for sand, pea, and cobble, respectively. Further images and descriptions of the streams can be found elsewhere. 71-73,75

The streams receive water from a constant-head reservoir supplied by groundwater; the average hydraulic residence time in the reservoir is approximately 3.5 d before reaching the head of the streams. The stream baseflow for this study was 0.8 L s<sup>-1</sup>. Prior to turning on the water for the experimental season, the streams were biologically "reset" by removing terrestrial organic matter (e.g., leaves) and benthic algae by hand. The top layer of the streambed substrate ( $\sim$ 2– 5 cm) was physically mixed to mobilize any remaining organic matter. The substrate was then returned to mostly flat topography aside from natural roughness features created by the substrate. After water flow was initiated, the streams were allowed to flow for at least 2 days prior to experiments to naturally flush any loose organic matter.

#### 2.3 Characterization of the aggregation behavior of nanoparticles

The aggregation behavior of P90 and E171 was analyzed using dynamic light scattering (DLS) and phase analysis light scattering (PALS) (NanoBrook Omni, Brookhaven Instrument Corporation, Holtsville, NY). DLS was used to measure changes in the hydrodynamic diameter (HD) over approximately 65 min. A solution of 10 mg L<sup>-1</sup> TiO<sub>2</sub> was prepared in either ultrapure water (18.2 M $\Omega$  cm), or unfiltered stream water (pH 8.12), filtered stream water (0.22 µm PTFE membrane). Immediately after adding the TiO2 to water, the samples were shaken vigorously and 3 mL was added to a plastic cuvette for DLS measurement. All measurements were conducted at a 90° scattering angle at 25 °C with a 10 s equilibration time. The HD was measured in triplicate and the average and standard deviation of the effective diameters were reported. PALS was used to measure the zeta potential ( $\zeta$ ) of P90 and E171 in the stream water. No background electrolyte was added to the solutions due to the already existing conductivity. 10 mg L<sup>-1</sup> solutions of TiO<sub>2</sub> were prepared in the filtered stream water and then mixed for 24 h. Samples were then diluted to ( $\sim 100~\mu g~L^{-1}$ ) and added to a plastic cuvette for analysis. Thirty measurement cycles were conducted at a 15° scattering angle and at 25 °C in triplicate, and the average and standard deviation were reported. The zeta potential was calculated from electrophoretic mobilities using Smoluchowski model (*i.e.*,  $\kappa a > 1$ ).

#### 2.4 Stream experiments

The stream-scale experiments were conducted in both June and September (2018). In June, immediately after the biological "reset", the biofilm growth was minimal and the streams

differed only by their streambed substrate. The streams were then allowed to freely colonize with biofilm throughout the remainder of the summer, resulting in a substantial growth of biofilms throughout each stream reach, as characterized previously.<sup>76</sup> Transport experiments were then repeated in September, during peak biofilm biomass (Fig. 2).

Stream transport and retention of NPs were investigated using short-term solute addition experiments with pulse injections (e.g., ref. 77). Before each experiment, background samples were taken every 10 m (i.e., 0, 10, 20, 30, 40, and 50 m). The pH, temperature, and conductivity were measured onsite, and water column samples were taken for further analyses, including total suspended solids (TSS), total dissolved solids (TDS), dissolved organic carbon (DOC), major ion concentrations, and background Ti. For TDS and TSS analysis, filters and crucibles were washed using water, then dried and weighed. 900 mL of stream water was then filtered through a 0.45  $\mu m$  nylon membrane followed by an ultrapure water rinse. The filter was dried in an oven at 105 °C for 1 h, placed in a desiccator for 10 min, and then weighed to measure TSS. The filtrate was placed in the crucible, dried in an oven overnight, placed in a desiccator for 10 minutes, and then weighed to measure TDS. DOC samples were filtered through a 0.45 µm nylon membrane, acidified, and analyzed using TOC-VCSH (Shimadzu, Addison, IL). Anion and cation concentrations were analyzed using ion chromatography (IC; ICS-5000, ICS 5000+, AS-23, CS-12A analytical columns, Thermo Scientific).

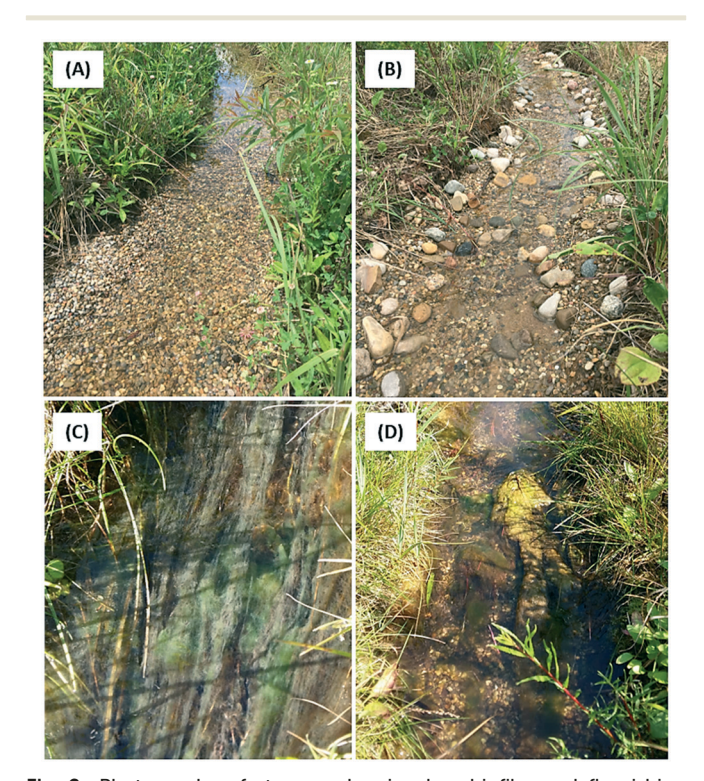


Fig. 2 Photographs of streams showing low biofilm and flourishing biofilm growth. (A) Pea stream with low biofilm, (B) mix stream with low biofilm, (C) pea stream with surface biofilms, and (D) pea stream with large biofilm sections. The stream width is 0.4 m.

Conservative tracers were used to evaluate the non-reactive transport behavior in the ND-LEEF streams in June and September, which corresponds to stream conditions with low and flourishing biofilms, respectively. In June, a solution of KBr (1 L of 500 mg L $^{-1}$ ) was used and samples were taken at 40 m downstream of the TiO $_2$  release point. In September, RWT (1 L of 11.48 mg L $^{-1}$ ) was used, and additional samples were taken at 20 m in addition to the 40 m point downstream to provide more detailed evidence of the transient transport behavior. The 1 L container of the RWT solution was covered with aluminum foil to prevent any degradation by the sunlight and vigorously shaken before release into streams. All tracer pulse injections were quickly poured right above the stream water surface.

For TiO<sub>2</sub> NP experiments, the P90 or E171 (1 L, 2 g L<sup>-1</sup>) pulse injections were rapidly released from a well-mixed container at the top of each stream. The NP solutions were prepared in ultrapure water and stirred for 24 h prior to stream injections, and solutions were vigorously shaken before release. To avoid cross contamination and minimize variations in the stream condition, the conservative tracers and TiO2 NPs experiments were conducted every other day (e.g., conservative tracer released on the first day, P90 released on the third day, E171 released on the fifth day, etc.). The volume and surface area of the substrate (i.e., ~3675 L of substrate in each stream) is much greater than the amount of TiO<sub>2</sub> used in each experiment, so influence from prior experiments would be minimal. Stream samples for NPs were collected using 50 mL conical centrifuge tubes (polypropylene, sterile, VWR, Batavia, IL) at 20 and 40 m from the release point at the top of the stream. All samples were taken in the channel thalweg, at approximately half the stream depth.

## 2.5 Quantification of conservative tracers and nanoparticles from stream experiments

Samples were transported to the lab and the concentration of bromide was measured using IC. A handheld fluorometer (DataBank<sup>TM</sup>, Turner Designs Inc., San Jose, USA) equipped with a Cyclops submersible sensor (Cyclops-7F, Turner Designs Inc.) was used for in situ measurements of the RWT concentration in the streams. Prior to using the fluorometer at ND-LEEF, the sensor was calibrated in the lab under dark conditions. When using the fluorometer, the sensor was placed at the 20 m point of each stream parallel to the streambed. The sensor was covered completely to prevent any penetration of sunlight that may interfere with the measurement of RWT. The fluorometer was programmed to measure RWT fluorescence every 2 seconds. At the 40 m point, RWT was sampled manually using 50 mL conical centrifuge tubes and stored in light-sealed container. The concentration was measured immediately experiment using the handheld fluorometer.

The concentration of Ti in the streams was measured using inductively coupled plasma with optical emission spectroscopy (ICP-OES; Perkin-Elmer Optima 8000,

PerkinElmer, Inc., Waltham, MA). A multi-element standard solution was (Inorganic Ventures, Christiansburg, VA, USA) was used for the quantification of Ti, and yttrium (Y) was used as an internal standard in the ICP-OES analysis. All sample concentrations were converted to TiO2 for reporting. Prior to ICP-OES analysis, samples were treated with microwave assisted acid digestion (Mars 6, CEM corporation, Matthews, NC) to dissolve TiO2 into Ti ions. An Se standard solution (SPEX CertiPrep, Metuchen, NJ, USA) was used as a surrogate to monitor the efficiency of the TiO2 acid-digestion. To prepare samples for the digestion, first, each TiO<sub>2</sub> sample was vigorously shaken for 3 min. Then, 5 mL of TiO2 sample was pipetted into a Teflon digestion vessel (PFA, CEM corporation, Matthews, NC), followed by adding 5 mL nitric acid (70%, trace metal grade, Fisher scientific, Hampton, NH). The microwave digestion protocol consisted of a 20 min temperature ramp to reach the target temperature 210 °C, which was then held for 45 min. Se (100 µL) was added with a nominal concentration of 100 mg L<sup>-1</sup> to every 20th Ti sample for quality assurance of the sample preparation process. After the digestion, all Ti and Se samples were prepared in ultrapure water with HNO<sub>3</sub> (<5% v/v) and analyzed with ICP-OES. The method detection limit (MDL) for P90 and E171, as calculated from eight replicates, was 2.1 and 6.3  $\mu$ g L<sup>-1</sup>, respectively.

#### 2.6 Analysis of breakthrough curves

The stream experimental data is plotted as a breakthrough curve (BTC), which describes the change in concentration as a function of time for a single point in the stream (*i.e.*, 40 m). Temporal moment analysis of the BTCs was used to evaluate mass transport behavior, calculated using the following equations for the 0th ( $M_0$ ), 1st ( $M_1$ ), and 2nd ( $M_2$ ) moments:<sup>78–80</sup>

$$M_0 = \int_0^t c(x, t) \mathrm{d}t$$

$$M_1 = \int_0^t tc(x, t) dt$$

$$M_2 = \int_0^t t^2 c(x, t) \mathrm{d}t$$

where, c(x, t) ( $M \cdot T \cdot L^{-3}$ ) is concentration at downstream location x and time t, Q is volumetric flowrate ( $L^3 \cdot T^{-1}$ ),  $M_0$  is the total area of the BTC, which is used to calculate the total mass recovery of NPs in the stream reach (*i.e.*, mass recovery or MR =  $M_0 \cdot Q$ ),  $M_1$  informs about the mean arrival time ( $T^2 \cdot M \cdot L^{-3}$ ),  $M_2$  provides information on the spread of the pulse injection as it advects downstream ( $T^3 \cdot M \cdot L^{-3}$ ). For analysis of the BTCs, we used the normalized 1st moment,  $M_1/M_0$ , which indicates the plume's mean arrival time (T), and the normalized central 2nd moment, which describes the variance (or plume spread) of the BTC, calculated as  $M_2/M_0 - (M_1/M_0)^2(T^2)$ . The integrals were estimated using the trapezoidal rule.

Environmental Science: Nano Paper

**Table 1** Background water quality characterization of ND-LEEF streams for June and September. All values are for a composite sample consisting of samples taken every 10 m in the stream (n = 6)

	Month	Sand	Pea	Cobble	Mix
Ionic strength (M)	Jun	0.017	0.017	0.017	0.017
	Sept	0.018	0.021	0.021	0.021
pН	Jun	8.22	8.12	8.16	8.19
	Sept	8.19	8.10	8.10	8.10
Conductivity (µS)	Jun	462	464	466	467
	Sept	544	547	547	547
TSS (mg L <sup>-1</sup> )	Jun	1.68	1.11	1.10	0.53
	Sept	1.60	2.61	3.56	0.84
TDS (mg L <sup>-1</sup> )	Jun	326	344	350	331
	Sept	397	407	398	397
DOC (mg L <sup>-1</sup> )	Jun	8.44	9.80	9.83	10.3
	Sept	12.4	10.9	12.2	11.4

Statistical analysis was done using a two-tailed paired two-sample mean t-test. Exact P values are reported, and significance was determined herein using an  $\alpha = 0.05$ .

#### 3. Results and discussion

# 3.1 Characterization of the stream and nanoparticle background parameters

Background environmental parameters (*i.e.*, ionic strength, pH, conductivity, TSS, TDS, and DOC) of the streams were analyzed in June and September (Table 1). Except for TSS and TDS, parameters differed by less than 5% between streams. Significant seasonal differences were observed for ionic strength (P = 0.023), conductivity ( $P = 1.1 \times 10^{-6}$ ), TDS (P = 0.001), and DOC ( $P = 8.3 \times 10^{-5}$ ). TDS and conductivity increased because the concentration of cations (e.g., Mg<sup>2+</sup> and Ca<sup>2+</sup>) and anions (Cl<sup>-</sup> and SO<sub>4</sub><sup>2-</sup>) increased (Table S1†),

and the increased DOC is likely a result of seasonal biofilm growth (i.e., Fig. 2).

Fig. 3 shows the change in the average HD for P90 and E171 prepared in ultrapure water, unfiltered stream water, and filtered stream water over approximately 65 min. After 30 s of mixing, the average HD of P90 in ultrapure water, unfiltered stream water, and filtered stream water was approximately 260  $\pm$  2.46 nm, 1130  $\pm$  94.8 nm, and 1200  $\pm$  113 nm, respectively. The average HD of E171 in these respective matrices after 30 s was  $300 \pm 6.85$  nm,  $486 \pm 11.5$  nm, and 510± 7.44 nm. The average primary particle size of P90 and E171 is approximately 16 nm (ref. 68) and  $106-132 \pm 38-56$  nm (n = 5 manufacturers<sup>69</sup>), respectively. Thus, the short-term DLS time-point results indicate that rapid aggregation occurred for both NPs using the primary particle size as a reference point, with more aggregation observed for P90 than E171. This agrees well with reported sizes for similar TiO2 NPs, where HDs reach approximately 200 to 300 nm in ultrapure water and 1200 to 1800 nm in high ionic strength water containing calcium, magnesium, and chloride ions. 46,81,82

After approximately 65 min of mixing, the average HD of P90 in ultrapure water, unfiltered stream water, and filtered stream water was approximately  $257 \pm 5.28$  nm,  $1940 \pm 179$  nm,  $2060 \pm 34.2$  nm, respectively. The average HD of E171 in these respective matrices after 65 min was  $384 \pm 107$  nm,  $480 \pm 18.2$  nm, and  $661 \pm 22.1$  nm. For P90 in ultrapure water, the HD did not increase beyond the first sample, but significant aggregation was observed for unfiltered (P = 0.003) and filtered (P = 0.015) stream water, with an HD nearly two-fold greater. For E171, the increase in HD for all matrices was minimal, with only the filtered sample showing any significant change (P = 0.011). These TiO<sub>2</sub> aggregation results agree with reported literature values.

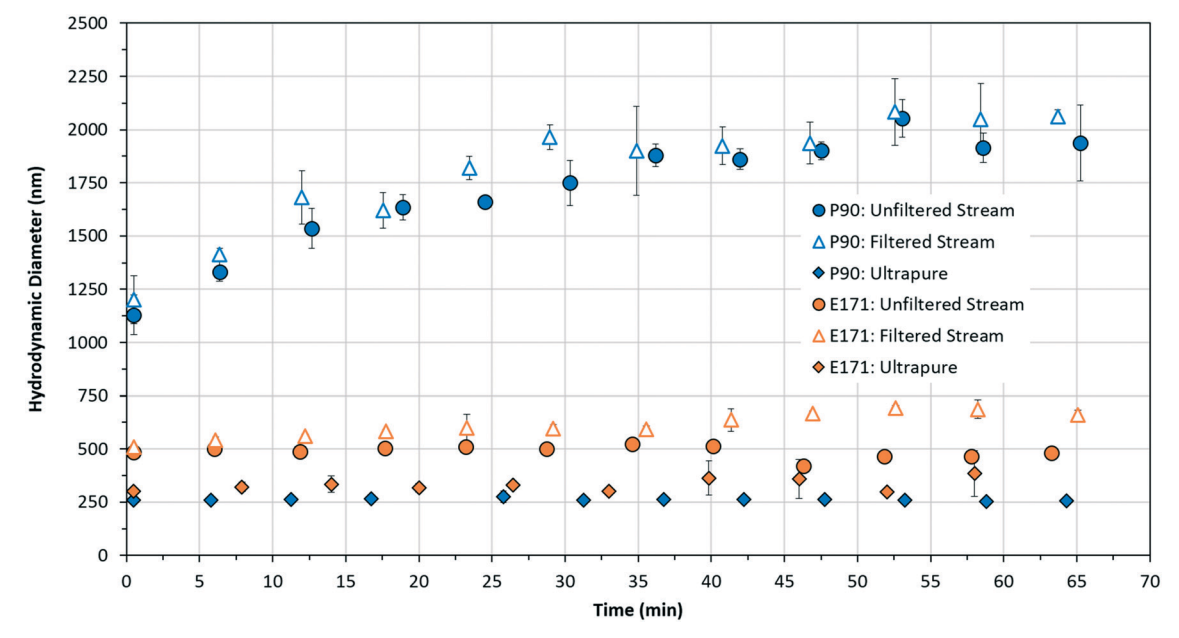


Fig. 3 The average hydrodynamic diameter as a function of time for P90 and E171 in unfiltered stream water, filtered stream water, and ultrapure water. The stream water was taken from the ND-LEEF site. The error bars represent the standard deviation of three analytical replicates.

For P90, there was no significant difference between filtered and unfiltered samples (P=0.36), indicating its size growth was dominated by homoaggregation and not heteroaggregation, which agrees with the relatively low TSS concentration in the streams (*i.e.*, Table 1). Though the HD of E171 was greater in the stream water than ultrapure water, it remained relatively stable over time compared to P90. This is due to the inherent negatively charged phosphates bound to the surface of E171(ref. 69) [*i.e.*,  $\zeta$  (P90)  $\approx$  -20 mV,  $\zeta$  (E171)  $\approx$  -40 mV in stream water; Fig. S2†], and this agrees with previous studies showing the increased stability of TiO<sub>2</sub> with adsorbed phosphates.<sup>83,84</sup>

## 3.2 Effect of the streambed substrate size on the transport of P90 and E171

The BTCs for the pulse injections of the conservative tracer, P90, and E171 during low biofilm growth conditions (June) are shown in Fig. 4, and results of the moment analysis are provided in Table S2.† Fig. 5 shows the mass recovery as a function of the mean arrival time for all experiments. For the tracers, the streambed order of mean arrival time and plume spread at 40 m was sand < mix  $\sim$  pea < cobble. For P90 and E171, the mean arrival time order at 40 m was sand < pea <

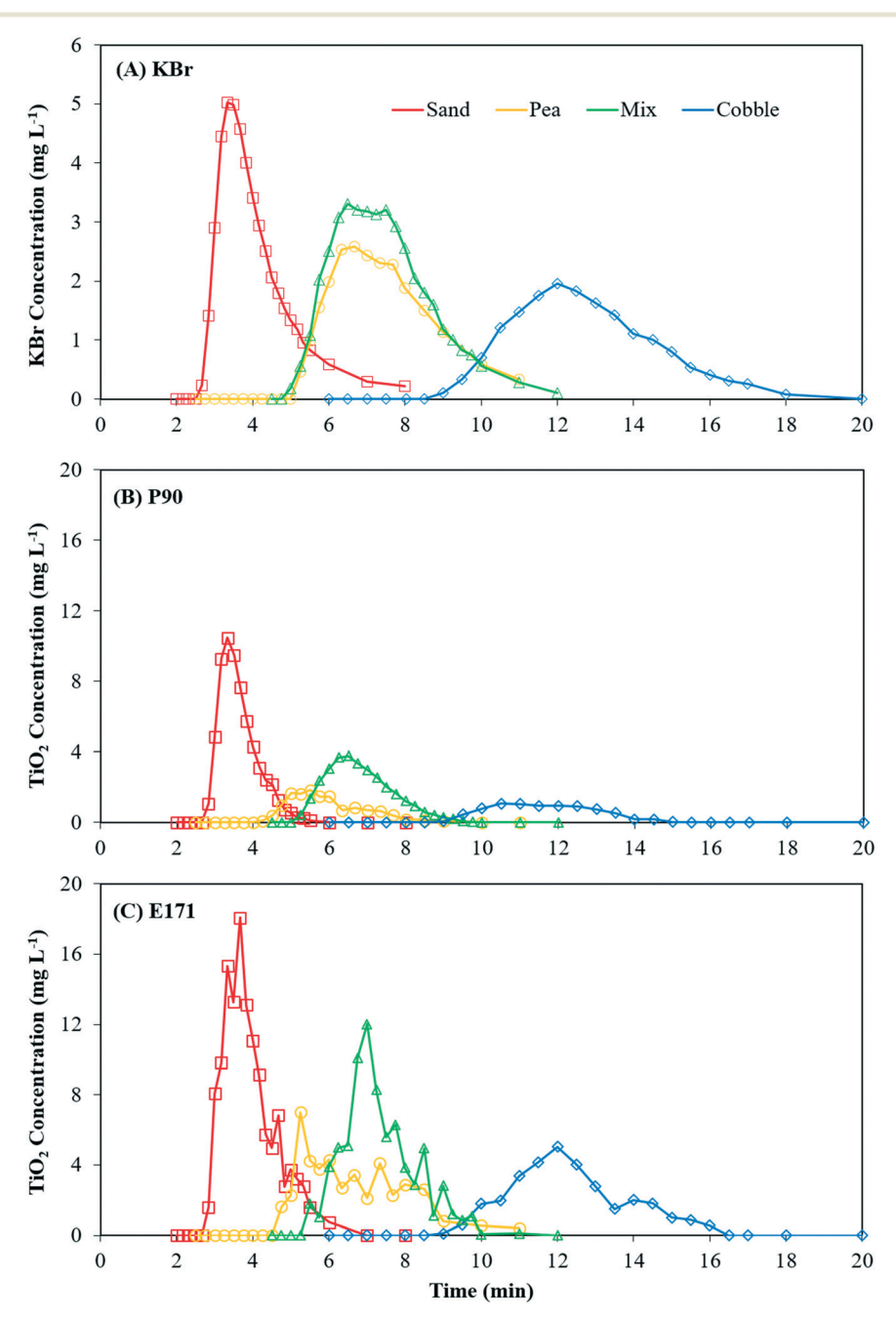


Fig. 4 BTCs of pulse injections for (A) the conservative tracer (KBr), (B) P90, and (C) E171. Experiments were conducted in June when biofilm growth in the stream was minimal. The BTCs represent samples taken at 40 m over a 20 min period.

Environmental Science: Nano Paper

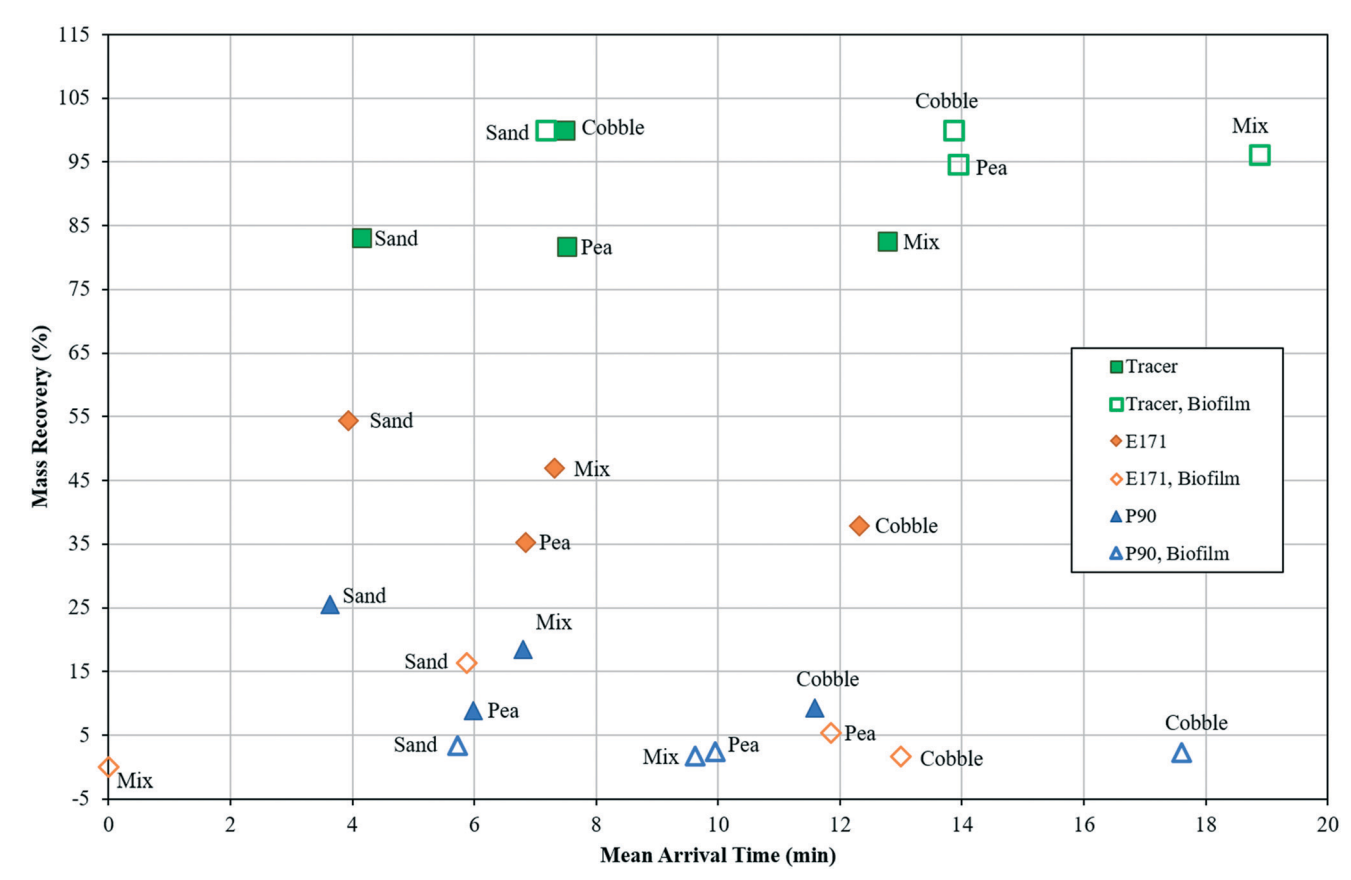


Fig. 5 Mass recovery as a function of the mean arrival time for the conservative tracers, P90, and E171. All data was taken from the breakthrough curves for the 40 m sampling point (i.e., Fig. 4 and 6). "Biofilm" indicates the September experiments when biofilms were flourishing.

mix < cobble, and plume spread order was sand < mix < pea < cobble. The trends were similar for the NPs and the conservative tracer, and there was a proportional relationship between the streambed substrate size and the arrival time and plume spread. This suggests that the transport of all samples was controlled by processes associated with streambed substrate size, including hyporheic exchange and in-stream dispersion due to variability in the substrate roughness. The mean arrival times increased with increasing substrate size so hyporheic exchange plays a major role in the transport behavior. Similar behavior has been observed for transport of kaolinite particles, where a considerably higher percentage of particles permeated through the pores of coarser sands compared to finer sands,85 which resulted in a reduced transport; however, contrasting behavior was observed for environmental DNA in the ND-LEEF streams.<sup>71</sup> The transport of environmental DNA was reduced in the finer streambed substrate compared to coarser substrate, which suggests that mechanical straining of the larger DNA fragments was the dominant retention mechanism. Rather, once exposed to the stream water, the NPs aggregated (i.e., Fig. 3), but transport was still fastest in the sand streams suggesting other mechanisms were responsible for the observed differences in the mean arrival time.

Though the mean arrival times for the NPs and the conservative tracer were similar for each stream, their mass

recoveries were notably different (Fig. 5 and Table S2†). For the conservative tracer, the mass recovery at 40 m was approximately 80% for sand, pea, and cobble and 100% for the mix stream. Presumably, the conservative tracer did not reach 100% mass recovery due to analytical detection limitations and experimental error. By comparison, the average mass recovery of P90 and E171 at 40 m for all streams was approximately 16% ± 8.0% and 44% ± 8.7%, respectively, and there was a significant difference between the NPs  $(P = 1.82 \times 10^{-5})$ . The order of decreasing mass recovery was sand > mix > cobble ~ pea. Because the mean arrival times for the NP and tracer were similar, but a reduction in mass recovery was observed, this suggests the NPs followed a similar flow pathway as the solute but were retained in the streambed substrate through either physical (e.g., straining) or chemical (e.g., adsorption) mechanisms. Likely, retention was due to a combination of both these mechanisms,26 which would be increased by NP aggregation in the stream. 8,10,41,46,86 Thus, the higher mass recovery observed for E171 was presumably due to its smaller aggregate size and more negatively charged surface, which would reduce straining and adsorption retention, respectively. The average  $\zeta$  of P90 and E171 in the stream water was approximately -20 and -40 mV (Fig. S2†), respectively. Typically, substrate such as sand is negatively charged, 46 and the negatively charged phosphate groups on

E171 would reduce adsorption through repulsive forces. Further, the increased magnitude of the  $\zeta$  would reduce the homoaggregation within the water column and pore water of the substrate, which may reduce immobilization by pore space settling. Thus, retention was greater in the larger substrate (*i.e.*, cobble) for both NPs because there was more hyporheic exchange with subsequent physical and chemical immobilization within the substrate.

#### 3.3 Effect of biofilm growth on the transport of P90 and E171

Pulse injection transport experiments were repeated in September after biofilms had flourished in the streams (i.e.,

Fig. 2). Biofilm growth was spatially heterogeneous along the streams, with visually observed variations in surface growth, thickness, and formation within the pore structure of the streambed substrate and biomass in the water column. Fig. 6 shows the BTCs for the tracer, P90, and E171 in the presence of enhanced biofilm growth, and the results of the moment analysis are provided in Table S2† with trends shown in Fig. 5. The overall transport behavior of the tracer and NPs was markedly different when biofilms were flourishing, with mean arrival times for nearly all conditions approximately 55–70% slower. The two notable exceptions were E171 in the cobble and mix streams, with approximately the same arrival time and no arrival observed, respectively. The increased

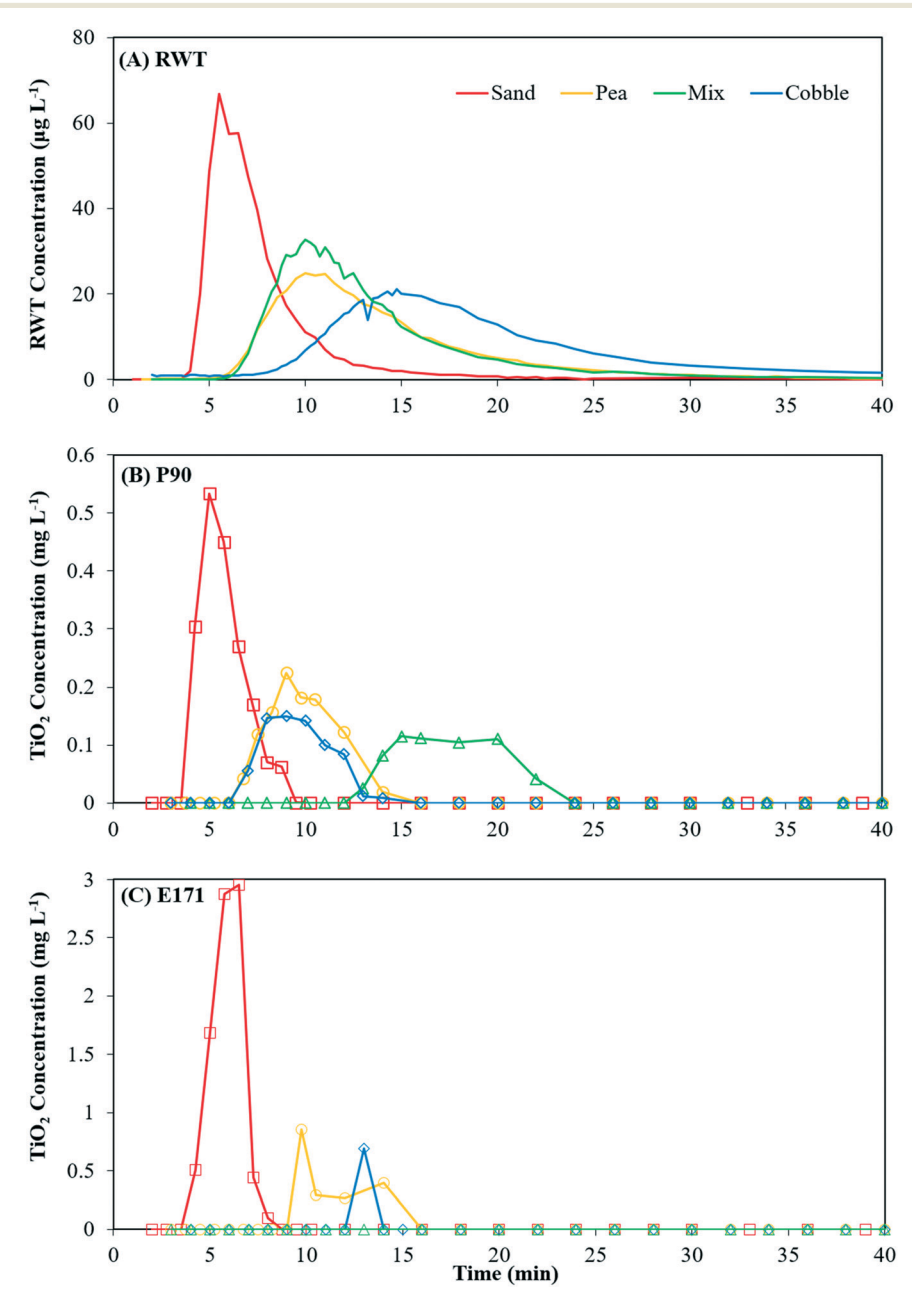


Fig. 6 BTCs of pulse injections for (A) the conservative tracer, (B) P90, and (C) E171. Experiments were conducted in June when biofilms were thriving. The BTCs represent samples taken at 40 m over a 40 m period. Sampling for the tracer was continuous (every 2 s).

Environmental Science: Nano

plume spread for the NPs was likely due to the increased mixing caused by the presence of biofilm structures in the water column and streambed. The increased mean arrival times could have been caused by many factors, including longer flow pathways and enhanced regions of recirculation.

Under these biofilm conditions, the average mass recoveries for all streams for the tracer, P90, and E171 were  $100 \pm 5.4\%$ ,  $2.4 \pm 0.7\%$ , and  $5.8 \pm 7.3\%$ , respectively. The large difference in mass recovery between the conservative tracer and the NPs indicates that the presence of biofilms caused retention of NPs, either through chemical or physical mechanisms. The mass recovery for NPs under flourishing biofilm conditions was significantly different compared to the mass recovery of the NPs under low biofilm conditions (P90, P = 0.041; E171, P = 0.0017). In fact, after experiments were completed, a visual inspection of the stream revealed obvious white sections of the biofilms where large amounts of the NPs had become trapped. Previous studies have also observed transfer of NPs to biofilms in various environmental settings.  $^{51,87}$ 

Additionally, the mass recovery difference between the two NPs became insignificant (P=0.38) when biofilms were present. Though the mass recovery for E171 was as high as 16.3% at 40 m in the sand stream, no mass recovery was observed for the mix stream. This dichotomy is presumably from the natural heterogeneous growth of biofilms in the streams, where large chunks of biofilm can attach to the side of the streams and remain in the water column (i.e. Fig. 2), which would allow retention of suspended NPs. This is supported by comparing mass recoveries between the 20 m

and 40 m sampling point for E171 in the sand stream. When biofilm growth was low, the mass recovery of E171 at the 20 and 40 m points was 60% and 54%, respectively. In comparison, when biofilms were flourishing, the mass recovery of E171 at the 20 and 40 m points was 44% and 16%, respectively. The decrease in mass recovery as E171 was transported downstream was more drastic under flourishing biofilm conditions, presumably due to the aforementioned heterogeneity. Similar results were observed for the pea stream (Table S2†).

#### 4. Conclusions

The results presented herein highlight the importance of hyporheic exchange and biofilm growth in controlling the transport of NPs in streams, and conceptual schematic of these processes is shown in Fig. 7. In streams where biofilm growth is minimal, transport of NPs will be controlled by mixing, hyporheic exchange, and the subsequent retention in the streambed substrate. When biofilms are flourishing, these will dominate immobilization of the NPs. The physico-chemical properties, especially the surface charge, of the NPs will affect aggregation and retention of NPs in the substrate, but this becomes less important in the presence of biofilms. Thus, in real streams, linking physico-chemical properties of pristine NPs to transport behavior may not be appropriate, as suggested previously.88 Future studies should move toward creating sophisticated models that can capture the inherent variability of the streams by coupling datasets from controlled field streams with labscale substrate transport experiments.

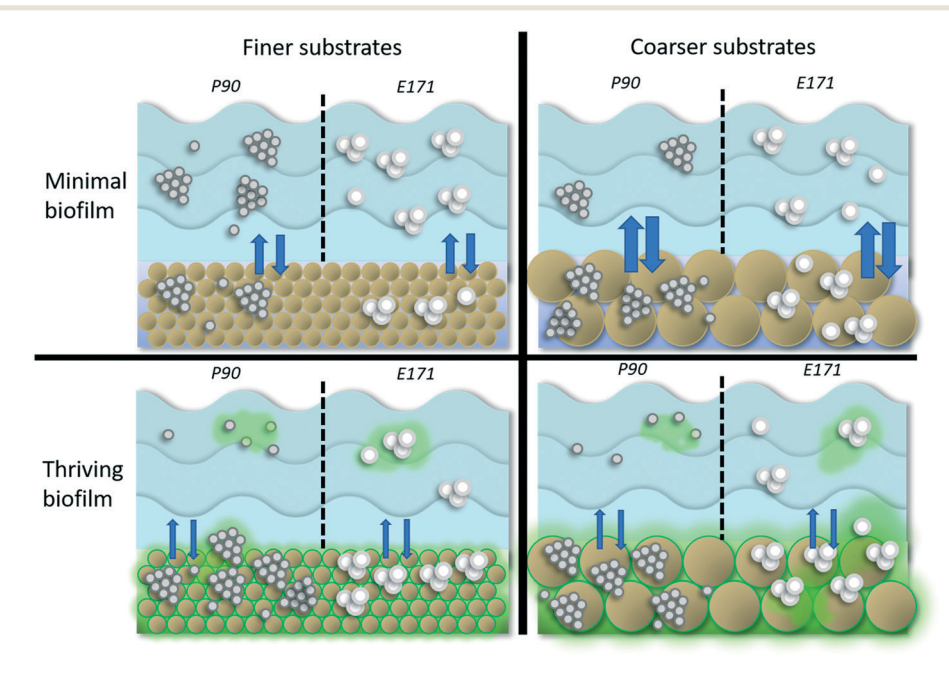


Fig. 7 Conceptualization of processes affecting NP transport in streams under the experiment conditions tested. Both NPs undergo homoaggregation in the streams, which is more severe for P90. Hyporheic exchange is greater for coarser substrates (indicated by the thickness of the vertical blue arrows). This allows for increased interaction between the NPs and the substrate resulting in increased retention. Biofilms can grow suspended in the water column, on the benthic layer, or within the pore spaces of the substrate. When biofilms are flourishing, hyporheic exchange is reduced, but they increase the retention of NPs and it is similar for P90 and E171 and across streams.

While this study is one of the first to our knowledge to present estimates of the transport of TiO2 NPs in field-scale streams with differing streambed substrate and biofilm conditions, there are limitations that exist due to experimental constraints. Foremost, experiments represented only a "pulse injection" scenario of a highly concentrated NP solution under relatively steady flow conditions. Likely, differing transport behavior will be observed with a continuous release of NPs to the streams, as observed previously for CeO2 NPs. 43 With a continuous release, the concentration of NPs will be lower and that may reduce aggregation and settling tendencies allowing for increased mobility. Nonetheless, downstream transport of NPs will likely be limited, and thus accumulation within the geological and biological media is to be expected near discharge points (e.g., wastewater treatment plant effluents). This chronic accumulation may cause localized negative effects on the streambed habitats, 89 with unintended negative consequences for stream ecological structure and function. 90 Additionally, storm events and higher flows are expected to cause resuspension of the NPs from the streambed substrate, 42 potentially moving them further downstream. The stream water used had relatively high ionic strength that was low in TSS and DOC. NP homoaggregation would be reduced in lower ionic strength waters, while higher TSS and DOC could enhance heteroaggregation and mobility, respectively. To enhance our understanding of NP transport in stream networks, further studies are needed with increased complexity at the field-scale involving geological collectors (e.g., clay particles), DOC, and organisms.

#### Conflicts of interest

There are no conflicts to declare.

## Acknowledgements

This material is based upon work supported by the National Science Foundation under grant no. CBET-1705770. Additional support for Mr. Junyeol Kim came from the CEST/Bayer Predoctoral Research Fellowship [Center for Environmental Science and Technology at Notre Dame (CEST)]. We especially want to thank the Notre Dame Environmental Change Initiation (ECI) for seed grant funding and ND-LEEF for use of the experimental streams. The authors thank CEST for access to instrumentation, including the IC, ICP-OES, and microwave digester. Lastly, we would like to thank Prof. Jennifer Tank and Mr. Brett Peters for their help setting up experiments at ND-LEEF.

#### References

1 Q. Zhang, J.-Q. Huang, W.-Z. Qian, Y.-Y. Zhang and F. Wei, The Road for Nanomaterials Industry: A Review of Carbon Nanotube Production, Post-Treatment, and Bulk Applications for Composites and Energy Storage, Small, 2013, 9, 1237–1265.

- 2 B. Pan and B. Xing, Applications and implications of manufactured nanoparticles in soils: a review, *Eur. J. Soil Sci.*, 2012, 63, 437–456.
- 3 M. F. L. De Volder, S. H. Tawfick, R. H. Baughman and A. J. Hart, Carbon Nanotubes: Present and Future Commercial Applications, *Science*, 2013, 339, 535.
- 4 Z. Fei Yin, L. Wu, H. Gui Yang and Y. Hua Su, Recent progress in biomedical applications of titanium dioxide, *Phys. Chem. Chem. Phys.*, 2013, 15, 4844–4858.
- 5 A. A. Keller, W. Vosti, H. Wang and A. Lazareva, Release of engineered nanomaterials from personal care products throughout their life cycle, J. Nanopart. Res., 2014, 16, 2489.
- 6 A. A. Keller, S. McFerran, A. Lazareva and S. Suh, Global life cycle releases of engineered nanomaterials, *J. Nanopart. Res.*, 2013, 15, 1692.
- 7 R. F. Domingos, N. Tufenkji and K. J. Wilkinson, Aggregation of Titanium Dioxide Nanoparticles: Role of a Fulvic Acid, *Environ. Sci. Technol.*, 2009, 43, 1282–1286.
- 8 E. M. Hotze, T. Phenrat and G. V. Lowry, Nanoparticle Aggregation: Challenges to Understanding Transport and Reactivity in the Environment, *J. Environ. Qual.*, 2010, 39, 1909–1924.
- 9 D. H. Lin, X. L. Tian, F. C. Wu and B. S. Xing, Fate and Transport of Engineered Nanomaterials in the Environment, J. Environ. Qual., 2010, 39, 1896–1908.
- 10 A. R. Petosa, D. P. Jaisi, I. R. Quevedo, M. Elimelech and N. Tufenkji, Aggregation and Deposition of Engineered Nanomaterials in Aquatic Environments: Role of Physicochemical Interactions, *Environ. Sci. Technol.*, 2010, 44, 6532–6549.
- 11 Y. G. Wang, Y. S. Li, H. Kim, S. L. Walker, L. M. Abriola and K. D. Pennell, Transport and Retention of Fullerene Nanoparticles in Natural Soils, *J. Environ. Qual.*, 2010, 39, 1925–1933.
- 12 T. Phenrat, J. E. Song, C. M. Cisneros, D. P. Schoenfelder, R. D. Tilton and G. V. Lowry, Estimating Attachment of Nano- and Submicrometer-particles Coated with Organic Macromolecules in Porous Media: Development of an Empirical Model, *Environ. Sci. Technol.*, 2010, 44, 4531–4538.
- 13 S. Torkzaban, Y. Kim, M. Mulvihill, J. M. Wan and T. K. Tokunaga, Transport and deposition of functionalized CdTe nanoparticles in saturated porous media, *J. Contam. Hydrol.*, 2010, 118, 208–217.
- 14 K. D. Hristovski, P. K. Westerhoff and J. D. Posner, Octanol-water distribution of engineered nanomaterials, *J. Environ. Sci. Health, Part A: Toxic/Hazard. Subst. Environ. Eng.*, 2011, 46, 636–647.
- 15 A. R. Petosa, S. J. Brennan, F. Rajput and N. Tufenkji, Transport of two metal oxide nanoparticles in saturated granular porous media: Role of water chemistry and particle coating, *Water Res.*, 2012, 46, 1273–1285.
- 16 D. X. Zhou, A. I. Abdel-Fattah and A. A. Keller, Clay Particles Destabilize Engineered Nanoparticles in Aqueous Environments, Environ. Sci. Technol., 2012, 46, 7520–7526.
- 17 J. A. Nason, S. A. McDowell and T. W. Callahan, Effects of natural organic matter type and concentration on the aggregation of citrate-stabilized gold nanoparticles, *J. Environ. Monit.*, 2012, 14, 1885–1892.

18 Y. Xiao and M. R. Wiesner, Transport and Retention of Selected Engineered Nanoparticles by Porous Media in the Presence of a Biofilm, *Environ. Sci. Technol.*, 2013, 47, 2246–2253.

Environmental Science: Nano

- 19 J. Yang, J. L. Bitter, B. A. Smith, D. H. Fairbrother and W. P. Ball, Transport of Oxidized Multi-Walled Carbon Nanotubes through Silica Based Porous Media: Influences of Aquatic Chemistry, Surface Chemistry, and Natural Organic Matter, *Environ. Sci. Technol.*, 2013, 47, 14034–14043.
- 20 M. T. Zhu, G. J. Nie, H. Meng, T. Xia, A. Nel and Y. L. Zhao, Physicochemical Properties Determine Nanomaterial Cellular Uptake, Transport, and Fate, Acc. Chem. Res., 2013, 46, 622–631.
- 21 Z. C. Qi, L. Hou, D. Q. Zhu, R. Ji and W. Chen, Enhanced Transport of Phenanthrene and 1-Naphthol by Colloidal Graphene Oxide Nanoparticles in Saturated Soil, *Environ.* Sci. Technol., 2014, 48, 10136–10144.
- 22 M. Zhu, H. T. Wang, A. A. Keller, T. Wang and F. T. Li, The effect of humic acid on the aggregation of titanium dioxide nanoparticles under different pH and ionic strengths, *Sci. Total Environ.*, 2014, 487, 375–380.
- 23 A. Praetorius, N. Tufenkji, K. U. Goss, M. Scheringer, F. von der Kammer and M. Elimelech, The road to nowhere: equilibrium partition coefficients for nanoparticles, *Environ.* Sci.: Nano, 2014, 1, 317–323.
- 24 E. Goldberg, M. Scheringer, T. D. Bucheli and K. Hungerbuhler, Prediction of nanoparticle transport behavior from physicochemical properties: machine learning provides insights to guide the next generation of transport models, *Environ. Sci.: Nano*, 2015, 2, 352–360.
- 25 A. L. Dale, G. V. Lowry and E. A. Casman, Much ado about alpha: reframing the debate over appropriate fate descriptors in nanoparticle environmental risk modeling, *Environ. Sci.: Nano*, 2015, 2, 27–32.
- 26 I. L. Molnar, W. P. Johnson, J. I. Gerhard, C. S. Willson and D. M. O'Carroll, Predicting colloid transport through saturated porous media: A critical review, *Water Resour. Res.*, 2015, 51, 6804–6845.
- 27 Y. Y. Sun, B. Gao, S. A. Bradford, L. Wu, H. Chen, X. Q. Shi and J. C. Wu, Transport, retention, and size perturbation of graphene oxide in saturated porous media: Effects of input concentration and grain size, *Water Res.*, 2015, 68, 24–33.
- 28 D. L. Karwan and J. E. Saiers, Hyporheic exchange and streambed filtration of suspended particles, *Water Resour.* Res., 2012, 48, 12.
- 29 F. Boano, J. W. Harvey, A. Marion, A. I. Packman, R. Revelli, L. Ridolfi and A. Worman, Hyporheic flow and transport processes: Mechanisms, models, and biogeochemical implications, *Rev. Geophys.*, 2014, 52, 603–679.
- 30 B. P. Espinasse, N. K. Geitner, A. Schierz, M. Therezien, C. J. Richardson, G. V. Lowry, L. Ferguson and M. R. Wiesner, Comparative Persistence of Engineered Nanoparticles in a Complex Aquatic Ecosystem, *Environ. Sci. Technol.*, 2018, 52, 4072–4078.
- 31 N. K. Geitner, N. J. O'Brien, A. A. Turner, E. J. Cummins and M. R. Wiesner, Measuring Nanoparticle Attachment

- Efficiency in Complex Systems, *Environ. Sci. Technol.*, 2017, 51, 13288–13294.
- 32 A. A. Markus, J. R. Parsons, E. W. M. Roex, P. de Voogt and R. Laane, Modelling the transport of engineered metallic nanoparticles in the river Rhine, *Water Res.*, 2016, 91, 214–224.
- 33 L. E. Barton, M. Auffan, L. Olivi, J. Y. Bottero and M. R. Wiesner, Heteroaggregation, transformation and fate of CeO2 nanoparticles in wastewater treatment, *Environ. Pollut.*, 2015, 203, 122–129.
- 34 J. Labille, C. Harns, J. Y. Bottero and J. Brant, Heteroaggregation of Titanium Dioxide Nanoparticles with Natural Clay Colloids, *Environ. Sci. Technol.*, 2015, 49, 6608–6616.
- 35 J. B. Liu, Y. S. Hwang and J. J. Lenhart, Heteroaggregation of bare silver nanoparticles with clay minerals, *Environ. Sci.: Nano*, 2015, 2, 528–540.
- 36 A. A. Markus, J. R. Parsons, E. W. M. Roex, P. de Voogt and R. Laane, Modeling aggregation and sedimentation of nanoparticles in the aquatic environment, *Sci. Total Environ.*, 2015, 506, 323–329.
- 37 A. Praetorius, J. Labille, M. Scheringer, A. Thill, K. Hungerbuhler and J. Y. Bottero, Heteroaggregation of Titanium Dioxide Nanoparticles with Model Natural Colloids under Environmentally Relevant Conditions, *Environ. Sci. Technol.*, 2014, 48, 10690–10698.
- 38 J. T. K. Quik, I. Velzeboer, M. Wouterse, A. A. Koelmans and D. van de Meent, Heteroaggregation and sedimentation rates for nanomaterials in natural waters, *Water Res.*, 2014, 48, 269–279.
- 39 I. Velzeboer, J. T. K. Quik, D. van de Meent and A. A. Koelmans, Rapid settling of nanoparticles due to heteroaggregation with suspended sediment, *Environ. Toxicol. Chem.*, 2014, 33, 1766–1773.
- 40 J. T. K. Quik, M. C. Stuart, M. Wouterse, W. Peijnenburg, A. J. Hendriks and D. van de Meent, Natural colloids are the dominant factor in the sedimentation of nanoparticles, *Environ. Toxicol. Chem.*, 2012, 31, 1019–1022.
- 41 T. Areepitak and J. H. Ren, Model Simulations of Particle Aggregation Effect on Colloid Exchange between Streams and Streambeds, *Environ. Sci. Technol.*, 2011, 45, 5614–5621.
- 42 N. T. Boncagni, J. M. Otaegui, E. Warner, T. Curran, J. H. Ren and M. M. F. De Cortalezzi, Exchange of TiO2 Nanoparticles between Streams and Streambeds, *Environ. Sci. Technol.*, 2009, 43, 7699–7705.
- 43 L. F. Baker, R. S. King, J. M. Unrine, B. T. Castellon, G. V. Lowry and C. W. Matson, Press or pulse exposures determine the environmental fate of cerium nanoparticles in stream mesocosms, *Environ. Toxicol. Chem.*, 2016, 35, 1213–1223.
- 44 N. K. Geitner, J. L. Cooper, A. Avellan, B. T. Castellon, B. G. Perrotta, N. Bossa, M. Simonin, S. M. Anderson, S. Inoue, M. F. Hochella, C. J. Richardson, E. S. Bernhardt, G. V. Lowry, P. L. Ferguson, C. W. Matson, R. S. King, J. M. Unrine, M. R. Wiesner and H. Hsu-Kim, Size-Based Differential Transport, Uptake, and Mass Distribution of Ceria (CeO2) Nanoparticles in Wetland Mesocosms, *Environ. Sci. Technol.*, 2018, 52, 9768–9776.

- 45 K. L. Garner and A. A. Keller, Emerging patterns for engineered nanomaterials in the environment: a review of fate and toxicity studies, *J. Nanopart. Res.*, 2014, 16, 28.
- 46 N. Solovitch, J. Labille, J. Rose, P. Chaurand, D. Borschneck, M. R. Wiesner and J. Y. Bottero, Concurrent Aggregation and Deposition of TiO2 Nanoparticles in a Sandy Porous Media, *Environ. Sci. Technol.*, 2010, 44, 4897–4902.
- 47 S. Arnon, L. P. Marx, K. E. Searcy and A. I. Packman, Effects of overlying velocity, particle size, and biofilm growth on stream-subsurface exchange of particles, *Hydrol. Processes*, 2010, 24, 108-114.
- 48 J. Fabrega, R. Zhang, J. C. Renshaw, W. T. Liu and J. R. Lead, Impact of silver nanoparticles on natural marine biofilm bacteria, *Chemosphere*, 2011, 85, 961–966.
- 49 J. Z. He, C. C. Li, D. J. Wang and D. M. Zhou, Biofilms and extracellular polymeric substances mediate the transport of graphene oxide nanoparticles in saturated porous media, *J. Hazard. Mater.*, 2015, 300, 467-474.
- 50 X. J. Jiang, X. T. Wang, M. P. Tong and H. Kim, Initial transport and retention behaviors of ZnO nanoparticles in quartz sand porous media coated with Escherichia coli biofilm, *Environ. Pollut.*, 2013, 174, 38-49.
- 51 K. J. Kulacki, B. J. Cardinale, A. A. Keller, R. Bier and H. Dickson, How do stream organisms respond to, and influence, the concentration of titanium dioxide nanoparticles? A mesocosm study with algae and herbivores, *Environ. Toxicol. Chem.*, 2012, 31, 2414–2422.
- 52 R. N. Lerner, Q. Lu, H. Zeng and Y. Liu, The effects of biofilm on the transport of stabilized zerovalent iron nanoparticles in saturated porous media, *Water Res.*, 2012, 46, 975–985.
- 53 M. Crampon, J. Hellal, C. Mouvet, G. Wille, C. Michel, A. Wiener, J. Braun and P. Ollivier, Do natural biofilm impact nZVI mobility and interactions with porous media? A column study, *Sci. Total Environ.*, 2018, 610, 709–719.
- 54 M. V. Wright, C. W. Matson, L. F. Baker, B. T. Castellon, P. S. Watkins and R. S. King, Titanium dioxide nanoparticle exposure reduces algal biomass and alters algal assemblage composition in wastewater effluent-dominated stream mesocosms, Sci. Total Environ., 2018, 626, 357–365.
- 55 T. J. Battin, F. V. D. Kammer, A. Weilhartner, S. Ottofuelling and T. Hofmann, Nanostructured TiO2: Transport Behavior and Effects on Aquatic Microbial Communities under Environmental Conditions, *Environ. Sci. Technol.*, 2009, 43, 8098–8104.
- 56 C. T. T. Binh, E. Adams, E. Vigen, T. Z. Tong, M. A. Alsina, J. F. Gaillard, K. A. Gray, C. G. Peterson and J. J. Kelly, Chronic addition of a common engineered nanomaterial alters biomass, activity and composition of stream biofilm communities, *Environ. Sci.: Nano*, 2016, 3, 619–630.
- 57 M. Button, H. Auvinen, F. Van Koetsem, B. Hosseinkhani, D. Rousseau, K. P. Weber and G. Du Laing, Susceptibility of constructed wetland microbial communities to silver nanoparticles: A microcosm study, *Ecological Engineering*, 2016, 97, 476–485.

- 58 M. A. Maurer-Jones, I. L. Gunsolus, B. M. Meyer, C. J. Christenson and C. L. Haynes, Impact of TiO2 nanoparticles on growth, biofilm formation, and flavin secretion in Shewanella oneidensis, *Anal. Chem.*, 2013, 85, 5810–5818.
- 59 A. Ozaki, E. Adams, C. Binh, T. Z. Tong, J. F. Gaillard, K. A. Gray and J. J. Kelly, One-Time Addition of Nano-TiO2 Triggers Short-Term Responses in Benthic Bacterial Communities in Artificial Streams, *Microb. Ecol.*, 2016, 71, 266–275.
- 60 A. Weir, P. Westerhoff, L. Fabricius, K. Hristovski and N. von Goetz, Titanium Dioxide Nanoparticles in Food and Personal Care Products, *Environ. Sci. Technol.*, 2012, 46, 2242–2250.
- 61 H. B. Shi, R. Magaye, V. Castranova and J. S. Zhao, Titanium dioxide nanoparticles: a review of current toxicological data, *Part. Fibre Toxicol.*, 2013, **10**, 33.
- 62 I. S. Sohal, K. S. O'Fallon, P. Gaines, P. Demokritou and D. Bello, Ingested engineered nanomaterials: state of science in nanotoxicity testing and future research needs, *Part. Fibre Toxicol.*, 2018, 15, 31.
- 63 W. Dudefoi, H. Terrisse, M. Richard-Plouet, E. Gautron, F. Popa, B. Humbert and M. H. Ropers, Criteria to define a more relevant reference sample of titanium dioxide in the context of food: a multiscale approach, *Food Addit. Contam.*, *Part A*, 2017, 34, 653–665.
- 64 J. J. Faust, K. Doudrick, Y. Yang, P. Westerhoff and D. G. Capco, Food grade titanium dioxide disrupts intestinal brush border microvilli in vitro independent of sedimentation, *Cell Biol. Toxicol.*, 2014, 30, 169–188.
- 65 Y. Yang, K. Doudrick, X. Y. Bi, K. Hristovski, P. Herckes, P. Westerhoff and R. Kaegi, Characterization of Food-Grade Titanium Dioxide: The Presence of Nanosized Particles, *Environ. Sci. Technol.*, 2014, 48, 6391–6400.
- 66 J. Kim and K. Doudrick, Emerging investigator series: protein adsorption and transformation on catalytic and food-grade TiO2 nanoparticles in the presence of dissolved organic carbon, *Environ. Sci.: Nano*, 2019, 6, 1688–1703.
- 67 R. Yusoff, M. H. Kathawala, L. T. H. Nguyen, M. I. Setyawati, P. Chiew, Y. S. Wu, A. L. Ch'ng, Z. M. Wang and K. W. Ng, Biomolecular interaction and kinematics differences between P25 and E171 TiO2 nanoparticles, *NANO*, 2018, 12, 51–57.
- 68 K. Doudrick, O. Monzón, A. Mangonon, K. Hristovski and P. Westerhoff, Nitrate Reduction in Water Using Commercial Titanium Dioxide Photocatalysts (P25, P90, and Hombikat {UV}100), *J. Environ. Eng.*, 2011, 423.
- 69 Y. Yang, K. Doudrick, X. Bi, K. Hristovski, P. Herckes, P. Westerhoff and R. Kaegi, Characterization of Food-Grade Titanium Dioxide: The Presence of Nanosized Particles, *Environ. Sci. Technol.*, 2014, 48, 6391–6400.
- 70 J. Kim and K. Doudrick, Emerging investigator series: protein adsorption and transformation on catalytic and food-grade TiO2 nanoparticles in the presence of dissolved organic carbon, *Environ. Sci.: Nano*, 2019, 6, 1688–1703.
- 71 A. J. Shogren, J. L. Tank, E. Andruszkiewicz, B. Olds, A. R. Mahon, C. L. Jerde and D. Bolster, Controls on eDNA movement in streams: Transport, Retention, and Resuspension, Sci. Rep., 2017, 7, 11.

Environmental Science: Nano Paper

- 72 A. F. Aubeneau, B. Hanrahan, D. Bolster and J. Tank, Biofilm growth in gravel bed streams controls solute residence time distributions, J. Geophys. Res.: Biogeosci., 2016, 121, 1840-1850.
- 73 A. F. Aubeneau, B. Hanrahan, D. Bolster and J. L. Tank, Substrate size and heterogeneity control anomalous transport in small streams, Geophys. Res. Lett., 2014, 41, 8335-8341.
- 74 C. L. Jerde, B. P. Olds, A. J. Shogren, E. A. Andruszkiewicz, A. R. Mahon, D. Bolster and J. L. Tank, Influence of Stream Bottom Substrate on Retention and Transport of Vertebrate Environmental DNA, Environ. Sci. Technol., 2016, 50, 8770-8779.
- 75 K. R. Roche, A. J. Shogren, A. Aubeneau, J. L. Tank and D. Bolster, Modeling Benthic Versus Hyporheic Nutrient Uptake in Unshaded Streams With Varying Substrates, J. Geophys. Res.: Biogeosci., 2019, 124, 367-383.
- 76 B. R. Hanrahan, J. L. Tank, A. J. Shogren and E. J. Rosi, Using the raz-rru method to examine linkages between substrate, biofilm colonisation and stream metabolism in open-canopy streams, Freshwater Biol., 2018, 63, 1610–1624.
- 77 R. J. O. Hall and J. L. Tank, Ecosystem metabolism controls nitrogen uptake in streams in Grand Teton National Park, Wyoming, Limnol. Oceanogr., 2003, 48, 1120-1128.
- 78 P. C. Leube, W. Nowak and G. Schneider, Temporal moments revisited: Why there is no better way for physically based model reduction in time, Water Resour. Res., 2012, 48, W11527.
- 79 A. J. Valocchi, Use of temporal moment analysis to study reactive solute transport in aggregated porous media, Geoderma, 1990, 46, 233-247.
- 80 V. Renu and G. S. Kumar, Temporal moment analysis of solute transport in a coupled fracture-skin-matrix system, Sadhana, 2014, 39, 487-509.
- 81 M. B. Romanello and M. M. F. de Cortalezzi, An experimental study on the aggregation of TiO2 nanoparticles

- under environmentally relevant conditions, Water Res., 2013, 47, 3887-3898.
- 82 R. A. French, A. R. Jacobson, B. Kim, S. L. Isley, R. L. Penn and P. C. Baveve, Influence of Ionic Strength, pH, and Cation Valence on Aggregation Kinetics of Titanium Dioxide Nanoparticles, Environ. Sci. Technol., 2009, 43, 1354-1359.
- 83 X. Y. Liu, G. X. Chen and C. M. Su, Effects of material properties on sedimentation and aggregation of titanium dioxide nanoparticles of anatase and rutile in the aqueous phase, J. Colloid Interface Sci., 2011, 363, 84-91.
- 84 P. Guo, N. Xu, D. Li, X. X. Huangfu and Z. L. Li, Aggregation and transport of rutile titanium dioxide nanoparticles with montmorillonite and diatomite in the presence of phosphate in porous sand, Chemosphere, 2018, 204, 327-334.
- 85 D. L. Karwan and J. E. Saiers, Hyporheic exchange and streambed filtration of suspended particles, Water Resour. Res., 2012, 48, W01519.
- 86 W. Zhang, J. Crittenden, K. G. Li and Y. S. Chen, Attachment Efficiency of Nanoparticle Aggregation in Aqueous Dispersions: Modeling and Experimental Validation, Environ. Sci. Technol., 2012, 46, 7054-7062.
- 87 J. L. Ferry, P. Craig, C. Hexel, P. Sisco, R. Frey, P. L. Pennington, M. H. Fulton, I. G. Scott, A. W. Decho, S. Kashiwada, C. J. Murphy and T. J. Shaw, Transfer of gold nanoparticles from the water column to the estuarine food web, Nat. Nanotechnol., 2009, 4, 441-444.
- M. C. Surette, J. A. Nason and R. Kaegi, The influence of surface coating functionality on the aging of nanoparticles in wastewater, Environ. Sci.: Nano, 2019, 6, 2470-2483.
- A. J. Boulton, Hyporheic rehabilitation in rivers: restoring vertical connectivity, Freshwater Biol., 2007, 52, 632-650.
- B. P. Colman, L. F. Baker, R. S. King, C. W. Matson, J. M. Unrine, S. M. Marinakos, D. E. Gorka and E. S. Bernhardt, Dosing, Not the Dose: Comparing Chronic and Pulsed Silver Nanoparticle Exposures, Environ. Sci. Technol., 2018, 52, 10048-10056.